A new look into the 2004 M6 Parkfield Earthquake sequence using an updated earthquake catalog

Miguel Neves (mjneves@gatech.edu)[1]; Zhigang Peng[1]; Guoqing Lin[2]; Junle Jiang[3]

[1]Georgia Institute of Technology, [2]University of Miami, [3]University of Oklahoma

2022 SCEC Annual Meeting
Group B, Poster #064

Introduction

We present the Parkfield Matched filter Relocated (PKD-MR) earthquake catalog, a new high-resolution catalog for the 2004 Mw 6 Parkfield earthquake sequence in Central California, spanning from November 6, 2003, to March 28, 2005. The new catalog contains 13914 earthquakes, about 3 times the events in the NCSN catalog, detected using high-quality seismic data recorded by the borehole High-Resolution Seismic Network with matched filter detection and relocated using differential travel-times.

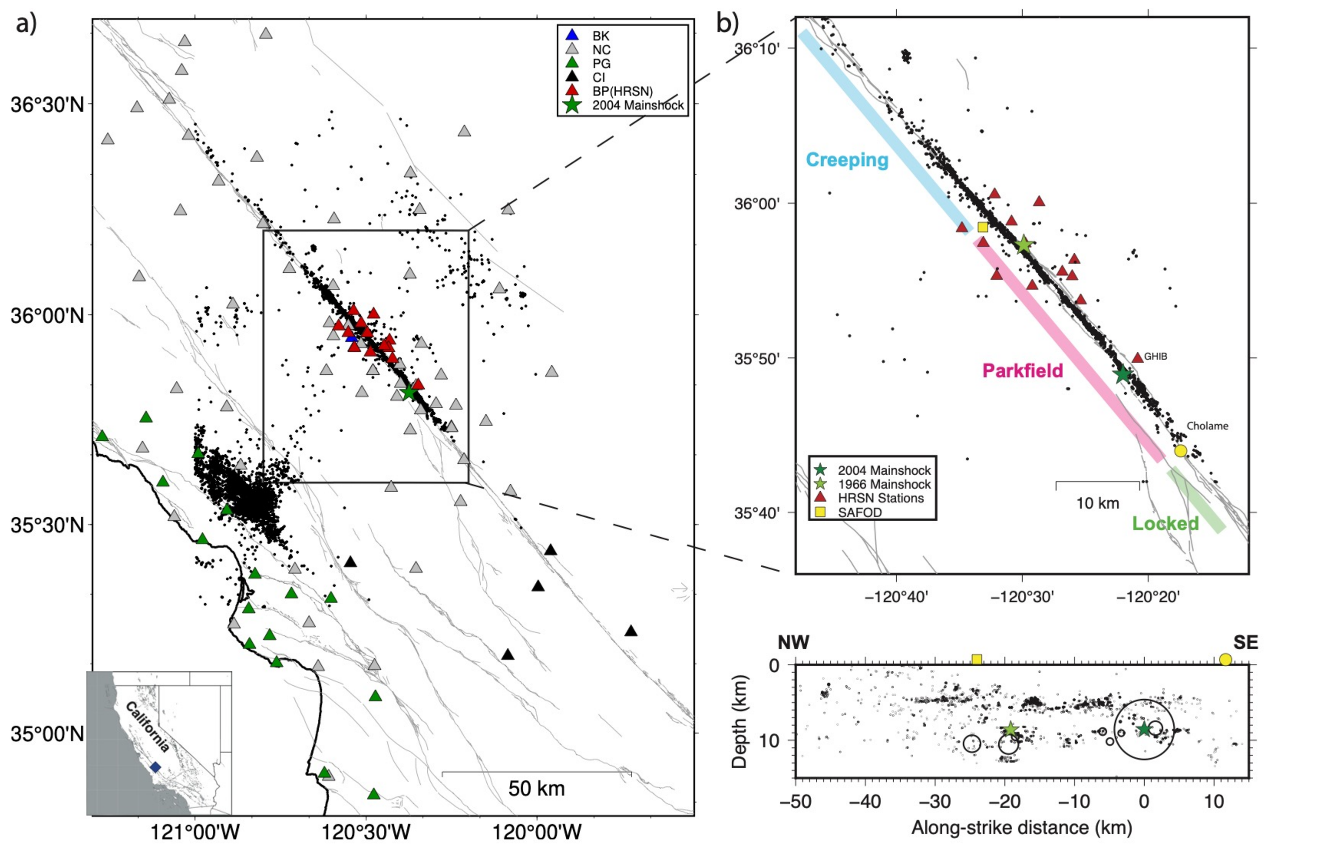

Figure 1: Study area in Central California. (a) Map of stations and templates used in our study. (b) Local templates and stations used for detection.

The PKD-MR catalog

The catalog was compiled using more than 10000 local and regional templates to perform matched filter detection on the 2-8 Hz frequency band. Detections were relocated using cross-correlation derived differential travel-times with XCORLOC (Lin, 2018). Magnitude was estimated computing the amplitude ratio between the detections and templates with a principal component fit (Shelly et al., 2016).

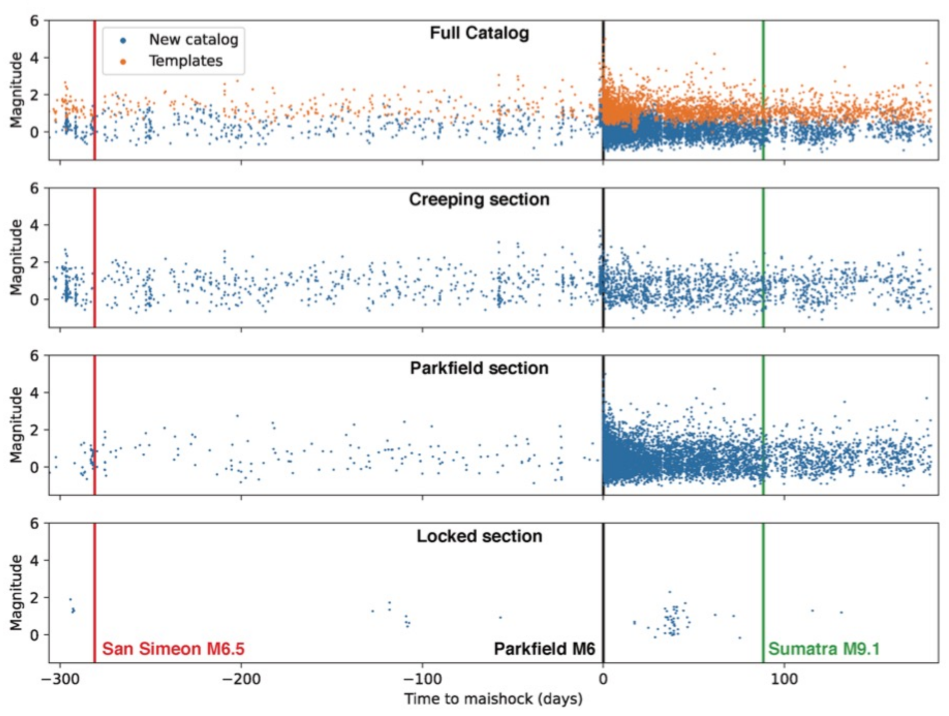

Figure 2: New relocated earthquake catalog. Earthquake magnitudes with time for the entire Parkfield segment and each of the fault sections. Marked by vertical lines are the times of three major earthquakes during the study period.

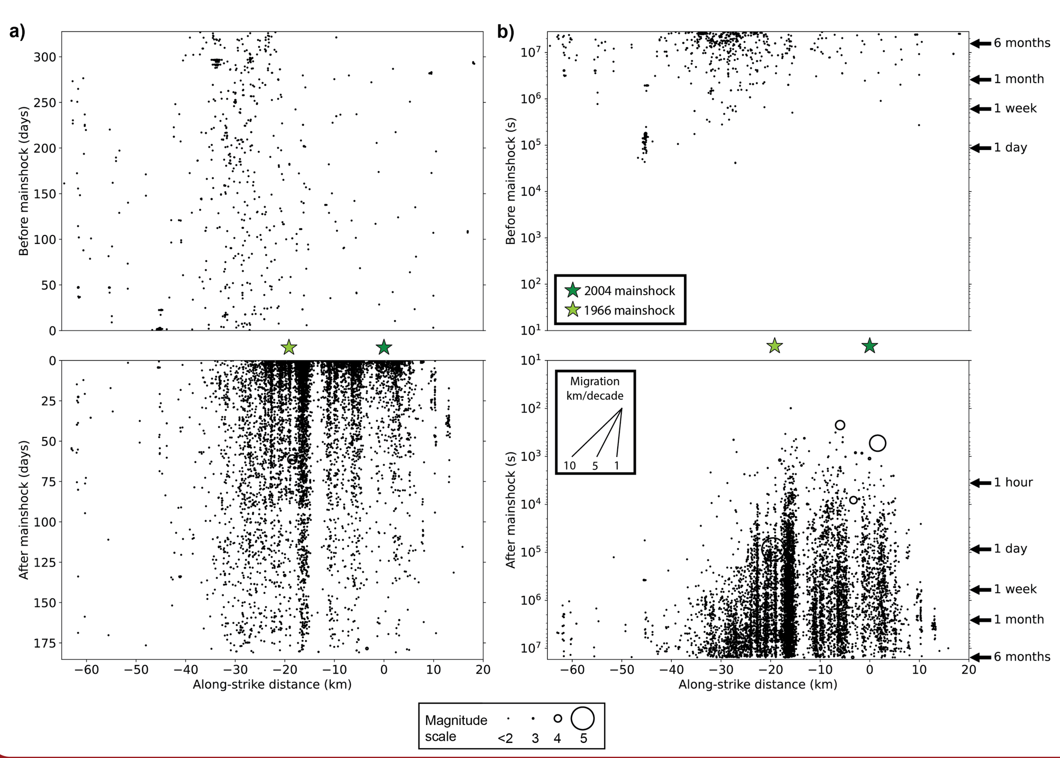

Figure 3: Along-strike distribution of the events in our relocated catalog with time.
a) Linear time scale.
b) Logarithmic time scale.

Precursory Signals

Analysis of seismic rate changes before the 2004 mainshock does not show clear precursory signals.

- We find a change in the seismic activity in the **Creeping section** of the San Andreas Fault (about ~30 km NW of the mainshock epicenter) in the weeks prior to the mainshock.
- **Parkfield section** activity remains stable in the months prior to the mainshock.

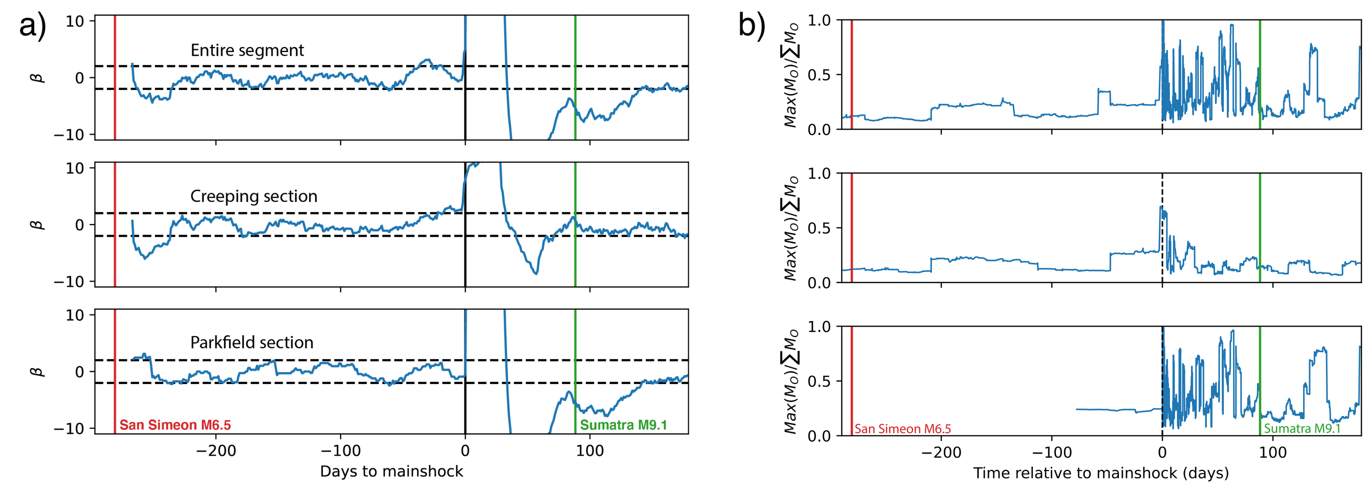

Figure 4: Variations in seismic activity. a) Seismic rate changes using β-statistics. b) Ratio of maximum seismic moment to total seismic moment. There is a significant seismic rate increase in the creeping section in the weeks prior to the mainshock.

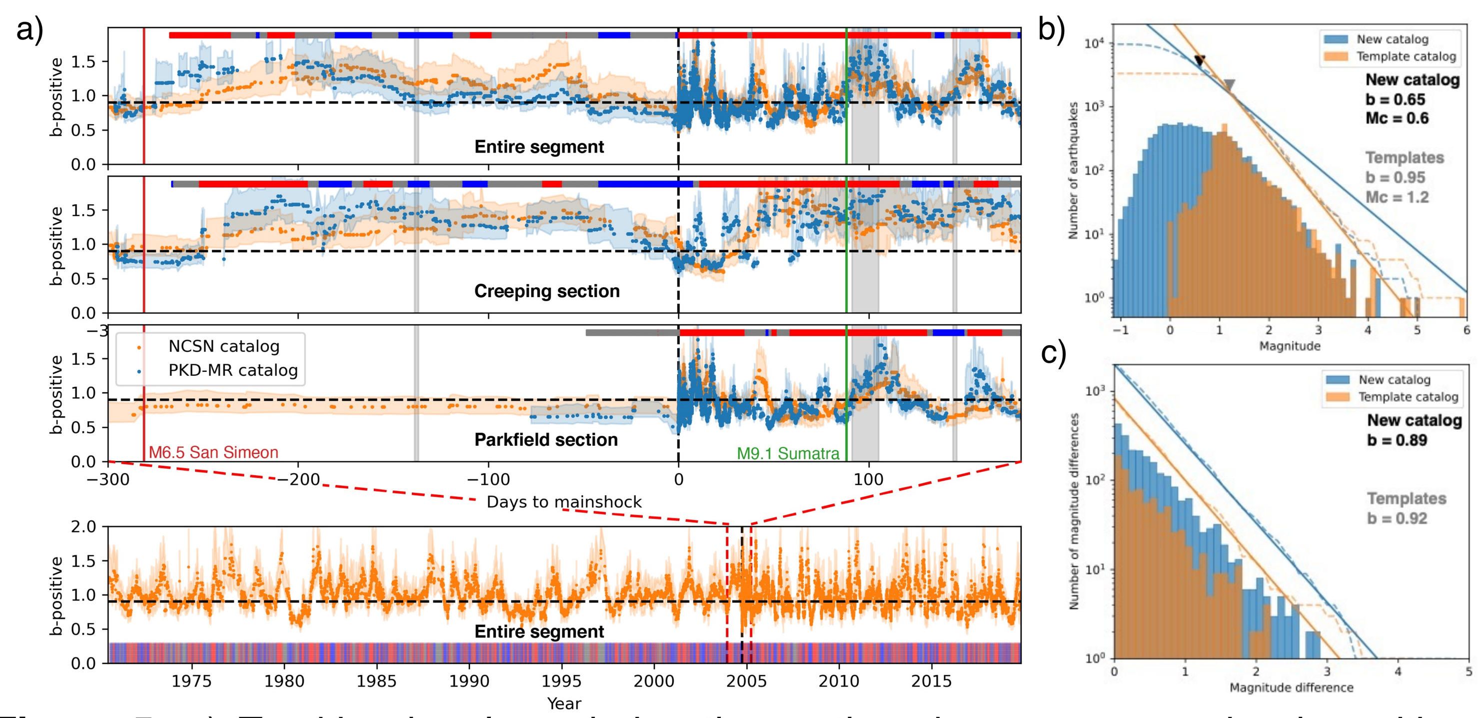

Figure 5: a) Tracking b-values during the earthquake sequence using b-positive estimator (van der Elst, 2021). Red, blue and gray bar shows significant positive, negative or no variations. b) Frequency magnitude distribution. c) Frequency magnitude difference distribution.

Aftershocks and Rheology

Using aftershocks and postseismic deformation information (Jiang et al., 2021) we estimate parameters for aftershock decay and the afterslip driven seismicity model by Perfettini and Avouac (2004) following Frank et al. (2017).

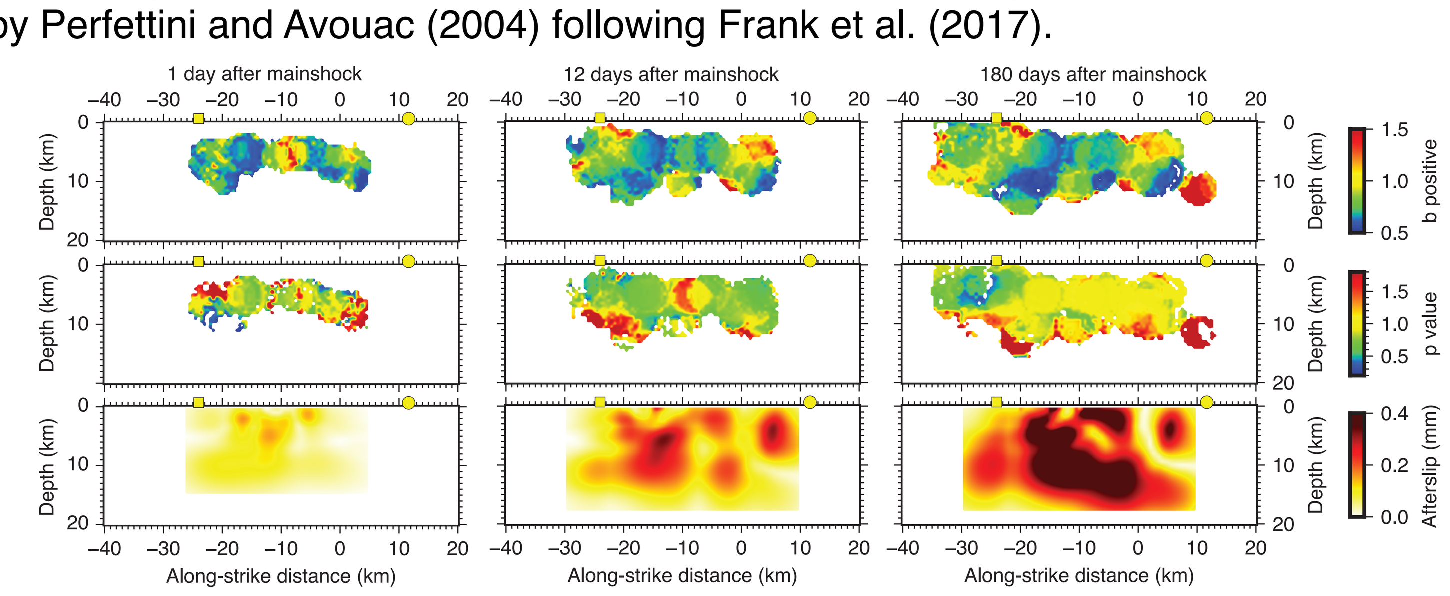

Figure 6: b-positive, Omori decay p-value and postseismic slip at different moments after the mainshock. Considering a 2 km radius using a 0.5x0.5 km grid.

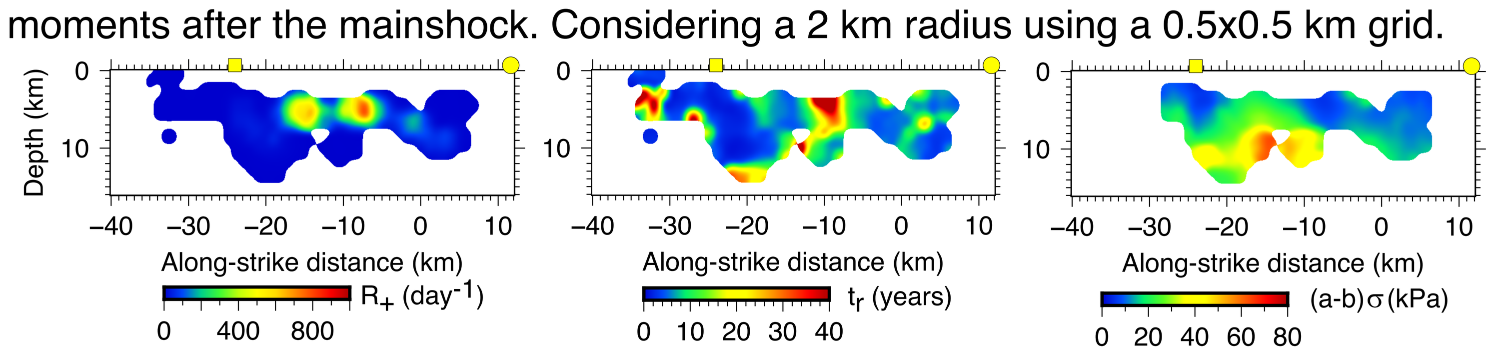

Figure 7: Using aftershocks to constrain rheology. t_r – relaxation time; R_+ – seismicity rate right after the mainshock; $(a-b)\sigma$ – rate and state parameter.

Tidal Stress Interactions

We use the new catalog to study interactions between tidal stresses and seismicity during the 2004 earthquake sequence. We find that seismicity:

- Before the mainshock is modulated by fortnightly tides and by semi-diurnal tides modulate only during the falling fortnightly tide.
- After the mainshock is modulated by semi-diurnal tides during both falling and rising fortnightly tide.

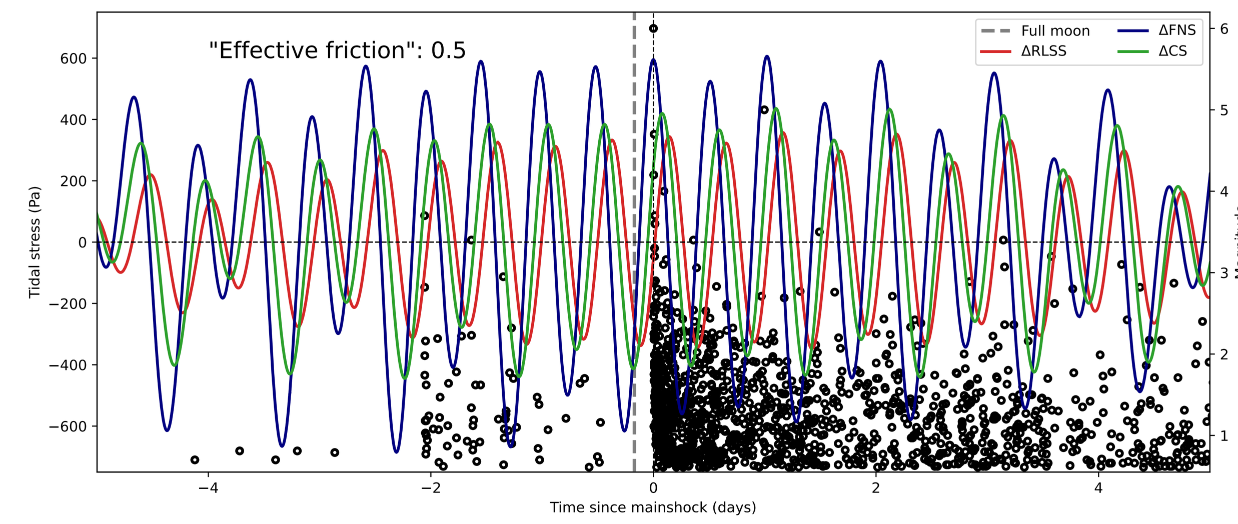

Figure 8: Modeled tidal stresses in the region using SPOTL (Agnew, 2012) and catalogued earthquakes above apparent magnitude of completeness. Blue – fault normal stresses; Red – right lateral shear stress; Green – Coulomb stress.

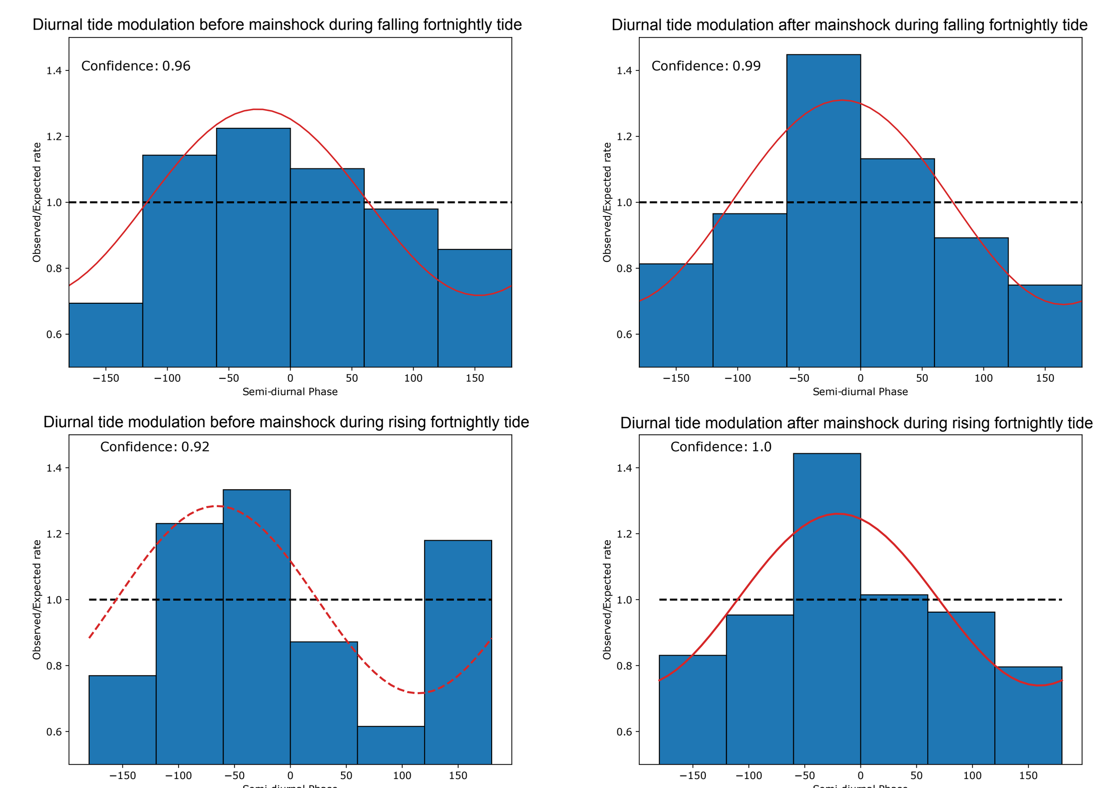

Figure 9: Modulation of seismicity with semi-diurnal tidal Coulomb stress phases. Solid red line shows statistically significant modulation, dashed red line not significant modulation.

Summary/Conclusion

- New PKD-MR earthquake catalog contains 13914 earthquakes, 3 times the number of events in the NCSN catalog.
- We identify a change in the seismic activity in the creeping section in the weeks prior to the mainshock.
- Tidal stresses modulate seismicity at Parkfield with different contributions before and after the mainshock.
- Using aftershock information we were able to map rheological parameters for the Parkfield segment.

References

- Neves, M., Peng, Z., and G. Lin (*in rev.*). A High-Resolution Earthquake Catalog for the 2004 M6 Parkfield Earthquake Sequence using a Matched Filter Technique.
- Agnew, D. C. (2012). SPOTL: Some Programs for Ocean-Tide Loading, SIO Technical Report, Scripps Institution of Oceanography.
- Frank, W. B., P. Poli, and H. Perfettini (2017). Mapping the rheology of the Central Chile subduction zone with aftershocks, *Geophysical Research Letters* **44**, no. 11, 5374–5382,.
- Jiang, J., Y. Bock, and E. Klein (2021). Coevolving early afterslip and aftershock signatures of a San Andreas fault rupture, *Science Advances* **7**, no. 15, eabc1606,.
- Lin, G. , 2018. The source-specific station term and waveform cross-correlation earthquake location package and its applications to California and New Zealand, Seism. Res. Lett.
- Perfettini, H., W. B. Frank, D. Marsan, and M. Bouchon (2018). A Model of Aftershock Migration Driven by Afterslip, *Geophysical Research Letters* **45**, no. 5, 2283–2293.
- Shelly, D. R., Ellsworth, W. L., & Hill, D. P. (2016). Fluid-faulting evolution in high definition: Connecting fault structure and frequency-magnitude variations during the 2014 Long Valley Caldera, California, earthquake swarm. Journal of Geophysical Research: Solid Earth.

Acknowledgements

The seismic data used in this work is available from the Northern California Earthquake Data Center. This work is supported by the National Science Foundation project EAR-1736197.
MN is supported by a PhD fellowship from the Portuguese research foundation FCT, grant SFRH/BD/139033/2018.